CLOUD CHAMBER INVESTIGATION OF THE ELECTRON-PHOTON COMPONENT NEAR THE AXIS OF EXTENSIVE AIR SHOWERS AT 3860 m ABOVE SEA LEVEL

T. V. DANILOVA, O. I. DOVZHENKO, S. I. NIKOL'SKII, and I. V. RAKOBOL'SKAIA

P. N. Lebedev Physical Institute, Academy of Sciences, U.S.S.R.

Submitted to JETP editor July 16, 1957

J. Exptl. Theoret. Phys. (U.S.S.R.) **34**, 541-547 (March, 1958)

The energy spectrum of the electron-photon component of extensive air showers was investigated at 3860 m above sea level at various distances from the axis. Showers with $\overline{N} = 1.5 \times 10^5$ were recorded. The fraction of high-energy electrons and photons recorded experimentally was appreciably smaller than that computed from cascade theory, especially at small distances from the axis. A better agreement between theory and experiment was obtained at larger distances. The lateral distribution of the energy carried by the electron-photon component can be approximated by the law r^{-n}, where $n = 1.5 \pm 0.3$ for distances from the shower axis in the range 1 — 9 m and for showers with $\overline{N} = 2 \times 10^5$.

IN continuation of the experiments of Ref. 1 we studied the spectrum of the electron-photon component in extensive air showers (EAS). The experiments were carried out in Autumn 1955 on Mt. Pamir (elevation 3860 m) by means of a rectangular cloud chamber[2] and a hodoscope consisting of about 1000 counters.[3] The chamber had a working volume of 60×60×30 cm and effective area equal to 0.15 m^2 for vertical showers. Seven lead plates, the first 0.5 cm thick, the second 1 cm, and the following five plates 1.5 cm each, were placed in the chamber. The top wall of the chamber was made of iron 1 cm thick.

EAS were selected by a coincidence-anticoincidence system consisting of several counter groups. The analysis of hodoscope data made it possible to find the axis position and the total number of particles for each shower.

Coincidences of discharges in four group of counters placed near the cloud chamber, 500 cm^2 in area each, were used for the selection of EAS. Anticoincidences between the central system and triple coincidences of three counter trays, 300 cm^2 in area each, placed at the vertices of a triangle at a distance of 19 m from the center of the array, were used in order to exclude showers with axes farther than 15 — 20 m from the center. In all, 300 showers with axes within a circle 9 m in radius were recorded.

Distribution of the recorded showers with respect to the number of particles is shown in Fig. 1.

The axis position and the total number of shower particles were found from the lateral distribution of charged particles determined by means of the hodoscope.[4] The error in axis location within 5 m from the cloud chamber was ≤ 1 m, for distances larger than 5 m the error amounted to 30 — 40%.

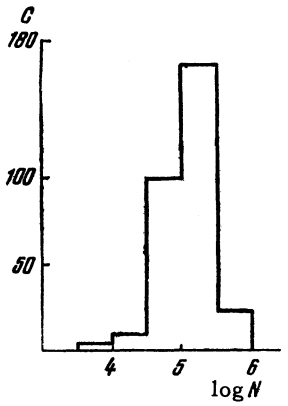

FIG. 1. Distribution of recorded extensive air showers with respect to the number of shower particles N. Number of showers recorded indicated on the y axis.

The energy of electrons and photons initiating a shower in the lead plates in the chamber was determined by comparing the total number of shower particles observed in the sections of the chamber with the number of particles calculated according to cascade curves for lead[5] (cf. Table I). The flux of particles propagating in the forward direction within the angle of 180° was considered. We did not differentiate between cascades produced by electrons and photons, since the visibility in the

TABLE I

E, ev	Section No.								ΣN
	1	2	3	4	5	6	7	8	
10^8	1.3	1.6	1.4	0.6	—	—	—	—	5
$2\cdot10^8$	1.8	2.8	2.7	1.3	0.4	—	—	—	9
$3\cdot10^8$	2.2	4.1	4.1	2.1	0.6	—	—	—	13
$4\cdot10^8$	2.5	5	5.2	2.8	1	0.4	—	—	17
$5\cdot10^8$	3	5.8	6.7	3.9	1.5	0.6	—	—	21.5
$6\cdot10^8$	3.4	6.3	8	4.9	2	0.6	0.4	—	25.6
$7\cdot10^8$	4	6.8	8.8	5.7	2.6	1.1	0.5	—	29
$8\cdot10^8$	4.5	7.2	9.3	6.5	3.2	1.5	0.7	—	33
$9\cdot10^8$	5	7.8	9.8	7.3	3.8	1.8	0.8	0.4	36.7
10^9	5.5	8.2	10.3	7.9	4.3	2.3	1.2	0.6	40.5
$2\cdot10^9$	6	12	17	16	12	6	3	2	74
$4\cdot10^9$	6.5	16	30	32	24.5	15	8	4	136
$6\cdot10^9$	8.5	24	42.5	48	37.5	24.5	13	7	205
$8\cdot10^9$	10	29	55.5	65	51.5	33	19	10	273
10^{10}	12.5	35	68.5	80.5	64	43	24.5	13	341

top section of the chamber was not always satisfactory and, besides, a considerable number of photons underwent conversion in the top wall of the chamber.

The accuracy of the energy measurement was 20 — 30% for the region $2 \times 10^8 - 2 \times 10^9$ ev. The high density of particles at higher energies (Fig. 2)

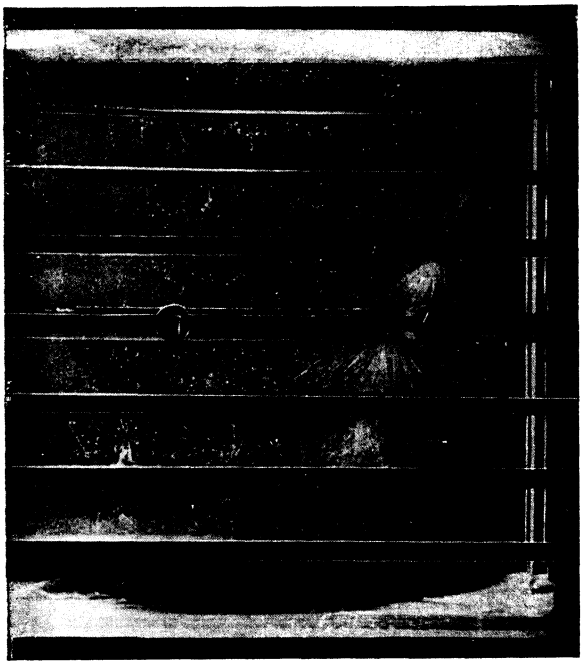

FIG. 2. Cascade shower produced in the chamber by a $\sim 10^{10}$ ev electron. The axis of the extensive air shower with $N = 1.3 \times 10^5$ fell ~ 0.8 m from the chamber.

made counting difficult and lowered the accuracy to 40 — 50%. For lower energies the accuracy was also worse because of the small number of secondary electrons.*

In 25 out of the 300 cases, the number of electrons and photons incident on the chamber was > 50. Showers produced by these particles were mixed together and difficult to separate. In these cases we found the shower cores, determined the maximum of the number of particles in each section and the number of plate in which the shower was absorbed, and comparing the results with the cascade curves, estimated the electron energy. The accuracy of energy determination was then slightly lowered. Five cases were not included in the final results because of the impossibility of separating the showers. The showers involved did not contain high-energy electrons and were characterized by a high particle flux density (~ 100) with energies $\leq 10^8$ ev.

The integral energy spectrum of electrons and photons for the region $10^8 - 10^{10}$ ev was measured for two distance intervals (0 — 4 and 4 — 9 m) for showers with the number of particles between $10^4 - 10^5$ ($\overline{N} = 6.4 \times 10^4$) and between $1.1 \times 10^5 - 10^6$ ($\overline{N} = 2 \times 10^5$). In the region $2 \times 10^8 - 10^9$ ev, the energy spectrum of the electrons and photons can be written in the form

$$N(\geqslant E) = \text{const} / E^{\gamma}.$$

The values of γ are given in Table II. In view of the absence of a marked dependence of γ on the

*Estimates of the accuracy of energy measurements were made under the assumption of a Poisson distribution of the number of particles at a given depth. Difficulties of a more exact treatment are connected with the problem of fluctuations of the number of particles in showers.

TABLE II

r	0–4 m		4–9 m	
$\bar{N}$	$6.4 \cdot 10^4$	$2 \cdot 10^5$	$6.4 \cdot 10^4$	$2 \cdot 10^5$
γ	0.63±0.07	0.60±0.06	1.3±0 3	1.3±0.3

number of particles in the shower, we grouped together showers with different number of particles for a more detailed analysis of the variation of the spectrum with the distance from axis. The results are given in Fig. 3.

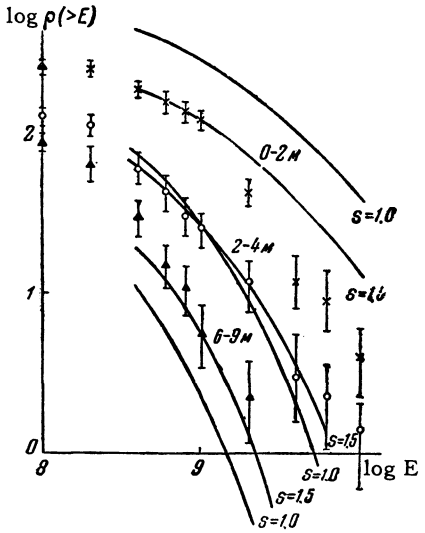

FIG. 3. Integral energy spectra of the electron-photon component of EAS in three distance intervals. Solid lines denote integral electron spectra computed from cascade theory for s = 1 and s = 1.5 (neglecting ionization losses). The experimental and the theoretical spectra are normalized for 10^9 ev and 2–4 m.

For comparison of the experimental results with the theoretical predictions we calculated the integral energy spectrum of electrons within a given distance interval for s = 1 and s = 1.5.* The function P(x, s) is tabulated in Ref. 7 for various values of s. The variable $x = Er_t/E_s$, where E is the electron energy in Mev, r_t is the distance from shower axis expressed in radiation units (at 3860 m one radiation unit is assumed to equal 460 m), and $E_s = 21$ Mev. The product $E^{2-s}P(x,s)$ is proportional to the number of particles with energy $\geq E$ at a given r. Integral energy spectra were calculated for s = 1 and s = 1.5 (the latter is shown in Fig. 4a). These were used for the calculation of the lateral distribution of electrons with energy $\geq E$ (Fig. 4b for s = 1.5),

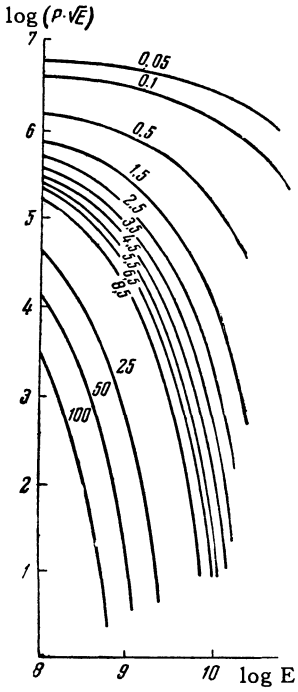

FIG. 4a

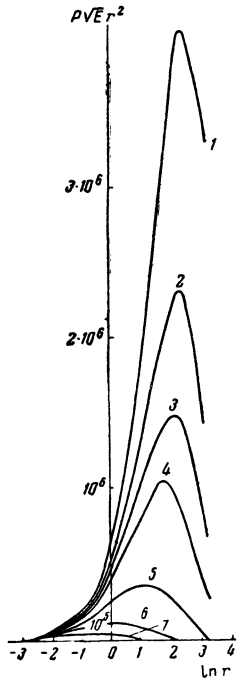

FIG. 4b

FIG. 4a. Integral energy spectrum of electrons at various distances from the axis for s = 1.5. The ordinates denote the decimal logarithm of the function $P\sqrt{E}$ proportional to the number of electrons with energy $\geq E$, the x axis – log E (E in ev). Numbers at the curves denote distance from the axis (m).

FIG. 4b. Lateral distribution of electrons with energy $\geq E$ for s = 1.5. Distance r in meters. The function $P\sqrt{E}$ is proportional to the number of particles with energy $\geq E$. The electron energies (in ev) are: 1 – 4×10^8, 2 – 6×10^8, 3 – 8×10^8, 4 – 10^9, 5 – 2×10^9, 6 – 6×10^9, 7 – 10^{10}.

which in turn were used for the determination of the number of electrons with energy $\geq E$ incident upon the area of the ring between the radii r_1 and r_2

$$N = 2\pi E^{2-s} \int_{r_1}^{r_2} P(x, s)\, r^2 d(\ln r).$$

Results of the calculations are shown in Fig. 3. The theoretical and experimental spectra are normalized for 10^9 ev at the distance of 2–4 m from shower axis. It can be seen from Fig. 3 that the experimental spectrum contains less high energy electrons near the axis. At larger distances this discrepancy practically disappears for the curve calculated for s = 1.5.

We calculated the ratio Δ of high-energy electrons and photons to the total number of particles in the shower for various distance intervals

*The value of s obtained from the absorption coefficient of shower particles in air is 1.2–1.3 (Ref. 6).

TABLE III

r, m	$\bar{N}$					
	Experimental values Δ, %				Theoretical values Δ, %	
	3860 m (1955)		100 m[1]	3260 m[6]	$s=1$	$s=1.5$
	$6.4\cdot10^4$	$2\cdot10^5$	10^4—$5\cdot10^4$	10^5—10^6		
0—2	(13±2)	(9±2)			38	15
2—4	(5.3±1.5)	(4±1)			12.5	8.5
0—4	(10±2)	(7±1.5)	(1.82±0.25)	~(11±5)	26	12
4—9	(4.2±2)	(2.0±0.5)		(5±3)	4.6	3.8

$$\Delta = \rho[E \geqslant 10^9,\ r_1,\ r_2] / \rho[E \geqslant 0,\ r_1,\ r_2].$$

where $\rho(E \geq 10^9) = N[E \geq 10^9, r_1, r_2]/C(r_1, r_2)\sigma$ is the density of electrons and photons with energy $\geq 10^9$ ev per m^2 in a shower falling within the given distance interval, $C(r_1, r_2)$ is the number of air showers in the given interval, σ is the effective area of the chamber for high-energy electrons and photons, and $N[E \geq 10^9, r_1, r_2]$ is the number of observed electrons with $E \geq 10^9$ ev in that interval. The value of $\rho(E \geq 0, r_1, r_2)$ was determined from hodoscope data. The ratio Δ determined from the experiment was compared with the results obtained from cascade theory for $s = 1$ and $s = 1.5$ under the assumption of an infinite energy of the primary particle. The results of the comparison are given in Table III and Fig. 5. It can be seen that the experiment yields a smaller fraction of high-energy electrons and photons than could be expected from cascade theory. The discrepancy is especially large for the distances 0 — 2 m for $s = 1$. This is in agreement, within the limits of the experimental errors, with the results of Hazen et al.[8] obtained by means of a cloud chamber at 3260 m above sea level. It should be noted that in Ref. 8 the electron energy was determined from the number of particles at cascade maximum and not from the sum of the number of particles in several points of the cascade curve as it was done in our work. The method used by Hazen is less accurate because of fluctuations and the energy values obtained are overestimated. Using that method, our value for Δ would be 13 — 14% instead of 10%.

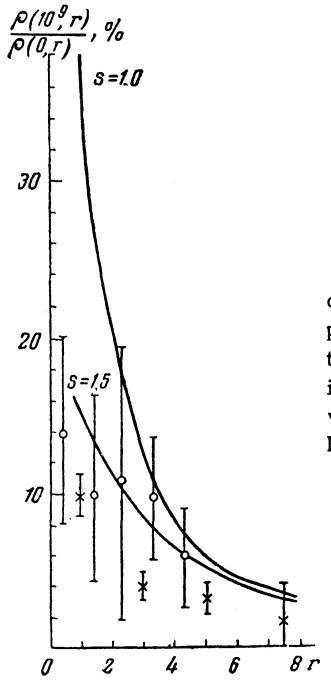

FIG. 5

FIG. 5. Ratio of the flux density of electrons and photons of $\geq 10^9$ ev to the total particle flux density in a given distance interval. o - denote data of Hazen,[8] × — of the authors.

A comparison was also made with the results of Ref. 1 (Table III). It can be seen that the fraction of high-energy electrons and photons found in experiments at 3860 and 3260 m elevation is larger than that at sea level[1] (the variation in the radiation length with altitude has been accounted for).

In 1957 we carried out new measurements with the cloud chamber at sea level, selecting events in which the EAS axis fell within 0 — 3 m from the chamber. The error in axis location amounted to ±1 m. The total number of particles in the studied showers was $\sim 10^4$. Showers of the same frequency and, evidently, the same primary energy, recorded at 3860 above sea level, have the total number of particles equal to $N = 6 \times 10^4$.*

Preliminary data indicate that the energy spectrum of electrons and photons measured at sea level coincide with that measured on the Pamir

*It can be assumed[6] that a shower of $N = 6 \times 10^4$ particles corresponds to a primary of $\sim 1.5 \times 10^{14}$ ev.

(Fig. 6), and the fraction of high-energy electrons and photons at sea level amounts to $\geq 10\%$.

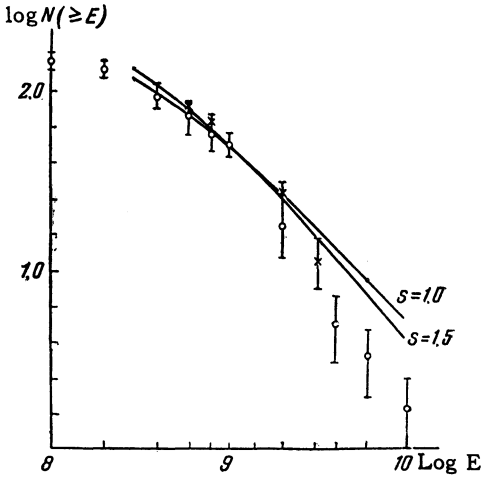

FIG. 6. Integral energy spectra of electrons and photons, × – at sea level, 0 – 4 m from axis, o – at 3860 m elevation, 0 – 4 m from axis. The curves represent calculations for two values of s.

At the present stage it is impossible to explain the discrepancy between the above results and those of Ref. 1. It is possible that it is partly due to the lower accuracy of shower axis location in the earlier experiments and to the larger amount of matter present in the roof of the laboratory where they were conducted. It is, however, possible that showers with different number of particles have different structure which causes the difference in the spectrum of the electron-photon component.

Using the results of the measurements at 3860 m it is possible to construct the lateral distribution of high-energy electrons and photons and the lateral distribution of the energy flux carried by the electron-photon component (ρ_E). In constructing the lateral distribution of the energy flux we accounted for electrons which did not initiate cascades in lead but which were absorbed in the first or second lead plate. Energy of such electrons was estimated from their ionization loss (cf. Ref. 1).

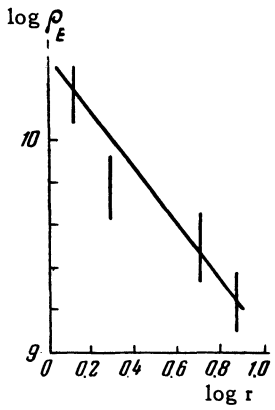

FIG. 7. Lateral distribution of the energy flux carried by the electron-photon component for showers with $\overline{N} = 2 \times 10^5$ (r in meters).

The dependence of $\overline{\rho}_E$ on r can be written in the form $\rho_E = r^{-n}$, where $n = 1.5 \pm 0.3$ for showers with $\overline{N} = 2 \times 10^5$ (Fig. 7).

In constructing the lateral distribution of high-energy electrons and photons the results were normalized for showers with $N = 10^5$ (Fig. 8). If we accept the value $s = 1.2$, then the lateral distribution of electrons and photons of $\geq 10^9$ and $\geq 2 \times 10^9$ ev cannot be explained by Coulomb scattering by air atoms only. This may be possibly connected with the influence of the angles of emission of π^0 mesons in nuclear interactions and of the lateral distribution of the nuclear-active component of EAS.

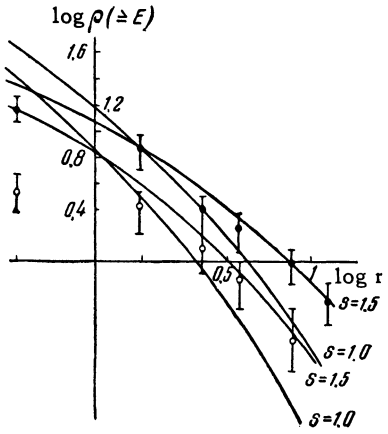

FIG. 8. Lateral distribution of electrons and photons with the energy ● – $E \geq 10^9$ ev, o – $E \geq 2 \times 10^9$ ev. Theoretical and experimental results are normalized for 10^9 ev at 1.5 m.

On the basis of the above experimental results one can, therefore, draw the following conclusions:

1. A deficiency of high-energy electrons and photons has been observed near the axis of EAS. This is evidently due to the presence of a flux of low-energy photons near the axis and also to the fact that nuclear-active particles of $10^{10} - 10^{12}$ ev contribute heavily to the production of the electron-photon component.

2. The spectrum of the electron-photon component of EAS produced by primaries of $\leq 2 \times 10^{14}$ ev does not vary with the altitude of observation. This fact can be explained either by equilibrium between the electron-photon component and the high-energy nuclear-active particles or by the preferential selection by the apparatus of EAS initiated at a certain effective altitude above the observation level.

In conclusion, the authors wish to express their gratitude to G. T. Zatsepin and L. I. Sarycheva for the discussion of results and to I. T. Uchaikin and D. F. Rakitin which took part in the measurements.

[1] Ivanovskaia, Kulikov, Rabobol' skaia, and Sarycheva, J. Exptl. Theoret. Phys. (U.S.S.R.) **33**, 358 (1957), Soviet Phys. JETP **6**, 276 (1958).

[2] I. A. Ivanovskaia and A. G. Novikov, J. Tech. Phys. (U.S.S.R.) **26**, 209 (1956); Soviet Phys. JTP **1**, 206 (1956).

[3] L. N. Korablev, Приборы и техника эксперимента (Instruments and Meas. Engg.) **2**, 54 (1956).

[4] Dovzhenko, Zatsepin, Murzina, Nikol' skii, Rakobol' skaia, and Tukish, Dokl. Akad. Nauk SSSR **118**, (1958).

[5] I. P. Ivanenko, Dokl. Akad. Nauk SSSR **107**, 819 (1956), Soviet Phys. "Doklady" **1**, 231 (1956).

[6] K. Greisen, Progress in Cosmic Ray Physics **3**, Amsterdam 1956, p. 1-14.

[7] V. V. Guzhavin and I. P. Ivanenko, Dokl. Akad. Nauk SSSR **115**, 1089 (1957), Soviet Phys. "Doklady" **2**, 407 (1957).

[8] Hazen, Williams, and Randall, Phys. Rev. **93**, 578 (1954).

Translated by H. Kasha
109

SOVIET PHYSICS JETP VOLUME 34 (7), NUMBER 3 SEPTEMBER, 1958

PECULIARITIES OF THE PHOTOCONDUCTIVITY IN CADMIUM SELENIDE

S. V. SVECHNIKOV

Kiev Polytechnic Institute

Submitted to JETP editor May 22, 1957

J. Exptl. Theoret. Phys. (U.S.S.R.) **34**, 548-554 (March, 1958)

Peculiarities of the photoconductivity in single crystals of cadmium selenide excited by red light of $\lambda = 7740$ A and by x-rays are considered. The first case corresponds to linear conductivity with a quantum yield $\beta^* = \text{const}$ and $\tau = \text{const}$, and the second case to nonlinear photoconductivity for which $\beta^* = \beta^*(L, J_{ph}, t)$ and $\tau = \tau(L, J_{ph})$. A two stage excitation scheme is proposed in order to explain the irregularities observed in the photoconductivity of single-crystal CdSe.

CADMIUM selenide as well as cadmium sulfide belong to those semiconducting materials with electron conductivity, which show a considerable internal photoeffect under the action of visible light as well as of other types of ionizing irradiation. From this point of view, CdSe can be quite effectively utilized for the preparation of photoresistors, whose integral sensitivity is measured in tens of amperes per lumen. With a resistance in the dark of more than 10^{14} ohms, changes in resistivity by a factor of $10^6 - 10^8$ are observed. The characteristics of the photoresistance are determined both by the technique of preparation as well as by the intrinsic properties of the semiconductor, whose internal photoeffect shows a number of peculiarities.

During the investigation of the properties of the added photoconductivity of single crystal CdSe, it was noted that the qualitative features of the internal photoeffect were similar for irradiation by visible light and by x-rays. This similarity shows up both in the statistical properties (current-voltage characteristics, nature of the light, variation of the sensitivity with applied bias, etc.) as well as in the transients in the photocurrent on switching the excitation in and out. The latter refers to the shape of the curve $J_{ph}(t)$ (Ref. 1), which determines the general features in the evolution of the process. Thus it is found that on approximating the rise and decay curves of the photocurrent by exponential functions, the time constants of these processes show the same dependence on the intensity of excitation, on the bias applied to the sample, on the temperature, etc., independent of whether the conductivity is stimulated by irradiation in the visible part of the spectrum or by x-rays. It was noted, however, that quantitatively the processes of excitation and decay of the photocurrent are substantially different in the two cases. Also, the detailed shapes of the curves prove to be different.

The samples investigated were single crystals